Colloids and Surfaces B: Biointerfaces 171 (2018) 320–326

Contents lists available at ScienceDirect

Colloids and Surfaces B: Biointerfaces

journal homepage: www.elsevier.com/locate/colsurfb

Interaction of green silver nanoparticles with model membranes: possible role in the antibacterial activity

Anike P.V. Ferreyra Maillard[a], Pablo R. Dalmasso[b,*,1], Beatriz A. López de Mishima[a], Axel Hollmann[c,d,*,1]

[a] INBIONATEC, CONICET, Universidad Nacional de Santiago del Estero, RN 9, Km 1125, 4206 Santiago del Estero, Argentina
[b] CIQA, CONICET, Departamento de Ingeniería Química, Facultad Regional Córdoba, Universidad Tecnológica Nacional, Maestro López esq. Cruz Roja Argentina, 5016 Córdoba, Argentina
[c] Centro de Investigaciones en Biofísica Aplicada y Alimentos (CIBAAL), CONICET, Universidad Nacional de Santiago del Estero, RN 9, Km 1125, 4206 Santiago del Estero, Argentina
[d] Laboratorio de Microbiología Molecular, Instituto de Microbiología Básica y Aplicada, Universidad Nacional de Quilmes, Roque Saenz Peña 352, B1876BXD Bernal, Argentina

ARTICLE INFO

Keywords:
Green silver nanoparticles
Lipid interaction
Surface pressure
Zeta potential
Interfacial adsorption

ABSTRACT

Silver nanoparticles (AgNPs) constitute a very promising approach for overcoming the emergence of antibiotic resistance bacteria. Although their mode of action could be related with membrane damage, the AgNPs-lipid membrane interaction is still unclear. In this sense, the present work investigated the interaction of model lipid membranes with AgNPs coated with different capping agents such as citrate (C-AgNPs) and phytomolecules (G-AgNPs) obtained *via* a green synthesis. The AgNPs-membrane interactions were evaluated studying i) the surface pressure changes on both zwitterionic (DMPC) and negatively charged (DMPC:DMPG) lipid monolayers, ii) the zeta potential and DLS of DMPC:DMPG liposomes and iii) Zeta potential on *Escherichia coli* membranes, incubated with this nanomaterials. The results showed that both negatively charged-AgNPs can interact with these lipid monolayers inducing an increase in the surface pressure but G-AgNPs presented a significantly higher affinity toward both monolayers in comparison with C-AgNPs. Zeta potential data confirmed again the interaction event showing that both DMPC:DMPG liposomes and *E. coli* bacteria became more negative with the addition of G-AgNPs. This increased net negative charge of the liposomes and *E. coli* allows to indicate an interfacial interaction where the green nanometal should keep adsorbed to the membrane *via* the insertion of aromatic/hydrophobic moieties of capping agents on the surface of AgNPs into the lipid bilayer. Summarizing, the AgNPs-membrane interaction should be an essential step in the antibacterial activity either because the membrane is the main target or by increasing the local concentration of silver from G-AgNPs accumulation which could cause the bactericidal effect.

1. Introduction

High prevalence of antibiotic resistance in human pathogens is a big challenge in both the pharmaceutical and biomedical fields and it leads to fear about the emergence and re-emergence of multi-drug resistance pathogenic and opportunistic microorganisms, mainly bacteria [1,2]. Thus, the rational development of new antimicrobial agents to improve bactericidal potential is a priority area of research in this modern era [3]. In the current scenario, nanotechnology offers new routes to take advantages of the antimicrobial behavior of known metals by synthesizing highly active metallic nanoparticles, in particular silver nanoparticles (AgNPs), to solve the problem of emergence of multi-drug resistance bacteria [4,5].

Even though silver is perhaps the oldest antimicrobial agent known by human being to fight infections and prevent spoilage [6], the use of silver in particles of nanoscale dimension with their novel and distinct physical, chemical, and biological properties is proving as an alternative for the development of new antibacterial agents [4,5]. However, in spite of the presence of many studies devoted to the antimicrobial activity of AgNPs, the mechanism of action and factors mainly affecting their antibacterial activity are still not well understood [7–9]. Several studies have proposed that AgNPs attach to the bacterial surface

* Corresponding authors.
E-mail addresses: p-dalmasso@hotmail.com (P.R. Dalmasso), ahollmann@conicet.gov.ar (A. Hollmann).
[1] Equal contributors, shared seniorship of the paper.

https://doi.org/10.1016/j.colsurfb.2018.07.044
Received 20 April 2018; Received in revised form 29 June 2018; Accepted 20 July 2018
Available online 21 July 2018

affecting its membrane properties. Likewise, it is possible that AgNPs can also penetrate inside the bacteria resulting in DNA damage. Another possible mechanism involved the dissolution of AgNPs releasing silver ions into the bacterial cell, which can affect a transcriptional response. [7]. Recently, AgNPs have also been shown to generate oxidative stress in *Staphylococcus aureus*, *Escherichia coli*, and *Pseudomonas aeruginosa* mediated by the increment of reactive oxygen species and a reduction of reactive nitrogen intermediates, which can lead to an oxidation of macromolecules like lipids, DNA, and proteins and consequently, the bacterial death [10].

In recent years, there is a growing interest to integrate green chemistry with the synthesis of AgNPs giving rise to novel design rules that are benign and eco-friendly. Thus, the biosynthetic approach using microorganism, fungi, and especially plant extracts has been proposed as a possible alternative to chemical and physical methods for the AgNPs production [10–13]. During the green synthesis of nanoparticles, functional biomolecules available in biological systems not only act as reducing agents instead of hazardous reductants but also act as eco-friendly capping agents in place of chemical ones. Moreover, it should be noted that green synthesized AgNPs (G-AgNPs) have shown better antibacterial properties than their chemically synthesized counterparts even though there was not much difference between their morphologies [14].

In this scenario, it is essential to study the interactions of G-AgNPs with model lipid membranes, which imitate the complexity of real cell membranes, and to extend the existing information in the literature on nanosilver-bacteria interaction for gaining insight into the mechanism of their antibacterial activity [15–19]. The present study contributes to a better knowledge of the interaction of lipid layers as a membrane-mimetic model with AgNPs coated with different capping agents such as citrate (C-AgNPs) and phytomolecules (G-AgNPs), which were obtained *via* a green chemical synthesis using the aqueous leaf extract of chicory (*Cichorium intybus* L.). Both surface pressure changes and zeta potential changes were used to characterize the nature of interaction of AgNPs with zwitterionic dimyristoylphosphatidylcholine (DMPC) and negatively charged dimyristoylphosphatidylcholine:dimyristoylphosphatidylglycerol (DMPC: DMPG) lipid monolayers, DMPC:DMPG liposomes, and *E. coli* bacteria. Although in recent years some studies have adopted other lipid mixtures including dimystoylphosphatidylethanolamine (DMPE):DMPG and cardiolipin (CL):DMPG, the most widely used DMPC:DMPG lipid mixture was employed as a model system to mimic the electrical properties of negatively charged bacterial outer membranes [20–25]. Moreover, the role of i) the AgNPs-lipid membrane interaction as an essential step in the mechanism of action of this nanomaterial, and ii) the nature of surface-capping ligands on the enhanced antibacterial activity of G-AgNPs is discussed.

2. Material and methods

2.1. Green synthesis and characterization of AgNPs

G-AgNPs were synthesized using a similar experimental method as previously reported [14]. Briefly, leaf pieces (5 g) of chicory obtained from a local market were boiled in 100 mL of ultrapure water for 5 min, and filtered to obtain the aqueous extract. Then, 5 mL of chicory leaf extract was added to 50 mL of 1 mM $AgNO_3$ solution with constant stirring at 75–80 °C for 15 min. C-AgNPs synthesis was performed using the well-known Turkevich method, which is based in the reduction properties of boiling citrate solutions. In brief, both a $AgNO_3$ solution and a citrate solution using a 1:1 Ag^+/citrate molar ratio were heated to boiling on a hot plate with continuous stirring for 30 min. $AgNO_3$ and sodium citrate were purchased from Cicarelli (Argentina) and used as received.

The formation of AgNPs was monitored by UV–vis spectroscopy using a Hewlett Packard 8453 diode-array spectrophotometer. The particle size distribution and colloidal stability of Ag-NPs were evaluated by dynamic light scattering (DLS) and zeta potential measurements, respectively, using a Horiba SZ-100 nanoparticle analyzer (Horiba, Kyoto, Japan). Furthermore, the morphological characterization of G-AgNPs was done using a JEM-JEOL 1120 EXII transmission electron microscope.

2.2. Screening for antibacterial activity of AgNPs

Antibacterial efficacy of both G-AgNPs and C-AgNPs was assayed using both the standard disk diffusion. Bacterial suspensions of *S. aureus* and *E. coli* adjusted to a turbidity of 0.5 McFarland scale were uniformly spread on Mueller Hinton (MH) agar (BritaniaLab) plates using a sterile cotton swab. After, filter paper disks impregnated with 10 µL of G-AgNPs or C-AgNPs at similar concentration were placed on MH agar plates. Plates were incubated for 24 h at 37 °C, followed by measurement of the diameter of inhibition zone in millimeters (mm), including the diameter of the filter paper disk [26].

2.3. Lipids

The zwitterionic lipid DMPC and negatively charged lipid DMPG were obtained from Avanti Polar Lipids (Alabaster, AL, USA). DMPC was chosen to mimic surface membrane of mammalian cells, as PC is the major component of mammalian cytoplasmic membranes, and because the lipid is stable to oxidation and readily hydrates in water forming lamellar phases at physiological pH and temperatures [27]. DMPG was chosen since phosphatidylglycerol is absent in eukaryotic plasma membranes, but is ubiquitous and abundant in bacterial membranes [27]. The ratio of PG:PG 5:1 was chosen in order to mimic in a simple way the bacterial membrane charge [20,21,28–30]. Large unilamellar liposomes/vesicles (LUV) were used trough the study. Briefly, multilamellar liposome vesicles (MLVs) were prepared by dissolving the pure lipids in chloroform, followed by evaporation under nitrogen flow to eliminate solvent traces. The dry lipid film was rehydrated by addition of 1 mL of 10 mM HEPES (Merck) buffer solution pH 7.4 and agitation at 45 °C for 1 h. LUV of 100 nm were prepared from MLVs by extrusion methods as described elsewhere [31,32].

2.4. Surface pressure

Changes on the surface pressure of lipid monolayers induced by AgNPs were measured in a Kibron Langmuir-Blodgett trough using DMPC or DMPC:DMPG (5:1) monolayers at constant temperature of (20.0 ± 0.5) °C. The surface of the HEPES buffer solution contained in a Teflon trough of fixed area was exhaustively cleaned by surface aspiration. Then, a solution of lipids in chloroform was spread on this surface to reach surface pressures of (20 ± 1) mN/m. Different concentrations of AgNPs were injected in the subphase and the surface pressure changes were recorded until a constant value was reached. Pressure data obtained were fitted with the following equation:

$$\theta = \frac{\Delta\Pi}{\Delta\Pi_{\max}} = \frac{[AgNPs]^n}{k_d + [AgNPs]^n} \quad (1)$$

where θ corresponds to the degree of coverage, ΔΠ is the surface pressure shift, [AgNPs] is the AgNPs concentration, n is the heterogeneity parameter describing the width of energy distribution, and k_d is the dissociation constant. In addition, the adsorption rate constant (k) was calculated from the following equation [33]:

$$\Delta\Pi = -e^{-kt}\Delta\Pi_{\max} + \Delta\Pi_{\max} \quad (2)$$

2.5. Electrophoretic mobility and zeta potential

Electrophoretic mobility of 1.25 mM DMPC:DMPG (5:1) liposomes incubated with different concentrations of G-AgNPs was determined in a Z-meter 3.0 (Zeta Meter Inc.) by applying a continuous electric field of

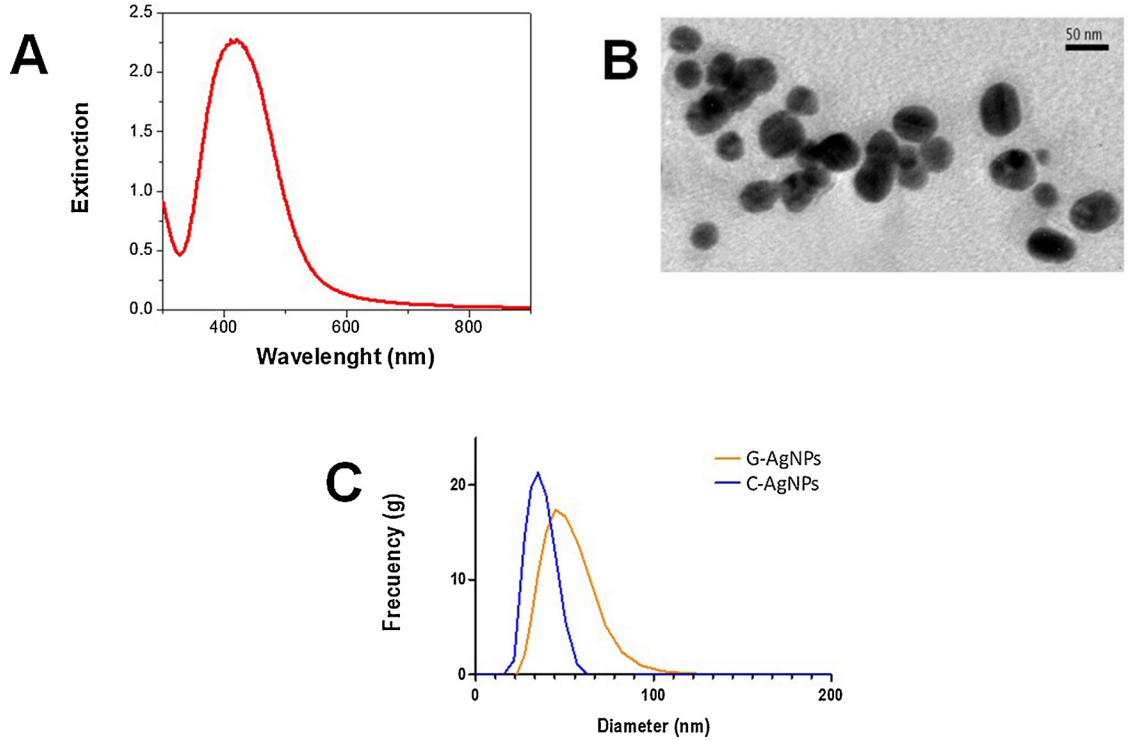

Fig. 1. A) Extinction spectrum of G-AgNPs. B) Representative TEM micrograph of G-AgNPs. C) Particle size of AgNPs determined by DLS.

40 V to a 100 nm extruded liposome suspension. The movement of the particle in the electrical field was followed by microscopic visualization in a reticulated objective. Values of the electrophoretic mobility (μ) were automatically given by the instrument. The zeta potential (ξ) in volts was calculated by the Smoluchowski equation:

$$\xi = 4\pi \times \frac{\eta \times \mu}{D} \quad (3)$$

where η is the viscosity of the suspension at 20 °C, D is the dielectric constant of the solution at 20 °C, and μ is the electrophoretic mobility of particles (micrometer/sec per volt/cm).

Zeta potentials were also determined to evaluate the interaction of G-AgNPs with a bacterial membrane using *E. coli* as model. The ones were measured with the help of a Horiba SZ-100 nanoparticle analyzer (Horiba Ltd). Suspensions of *E. coli* were obtained from the 24 h bacterial cultures growing in MH broth (BritaniaLab) at 37 °C. Bacterial suspensions with OD_{600} = 1.0 were injected with different concentrations of G-AgNPs and incubated for 1 h at 37 °C. After incubation, the suspensions were diluted twenty times and their zeta potentials were recorded.

2.6. Dynamic Light Scattering (DLS)

DLS experiments on G-AgNPs, DMPC:DMPG (5:1) LUVs, and a mixture of 1.25 mM of LUVs with 0.04 nM of G-AgNPs, were carried out on a Horiba SZ-100 nanoparticle analyzer with a scattering detection at 90° equipped with a DPPS laser (λ = 532 nm) at 25 °C, using disposable polystyrene cells. Normalized intensity autocorrelation functions were analyzed using the CONTIN method [34,35], yielding a distribution of diffusion coefficients (D). The measured D is used for the calculation of the hydrodynamic diameter (D_h) through the Stokes-Einstein relationship:

$$D_h = \frac{kT}{3\pi\eta D} \quad (4)$$

where k is the Boltzmann constant, T the absolute temperature, and η the medium viscosity. The D_h of the sample was obtained from the peak with the highest scattered light intensity in light scattering intensity distributions. For all determinations, normalization by the scattering light intensity mode and polydispersion distribution was chosen from the software options.

2.7. Data analysis

Fitting of the equations mentioned in this work to the experimental data was done by non-linear regression using GraphPad Prism 5. Error bars on data presentation represent the standard error of mean (SEM).

3. Results and discussion

Nanotechnology advances to modify the properties of metal in the form of nanoparticles appear to revive the use of AgNPs for biomedical applications, which have proved to be a powerful new generation of antimicrobial agents against a broad range of microbes including multidrug resistance bacteria [4,5]. While the toxic effects of silver on bacteria have been investigated for more than 60 years [6,36], the action mode of AgNPs on the bacteria is still unknown, being suggested possible mechanisms of action according to the morphological and structural changes in the bacterial cells [8,9,37], where AgNPs accumulated in the bacterial membrane caused the permeability, resulting in cell death. Although this event involves some type of binding mechanism, the mechanism of interaction between AgNPs and the outer membrane components is still unclear. In this context, the aim of the present work is the biophysical characterization of the interactions of lipid membranes with AgNPs coated with phytomolecules (G-AgNPs) or citrate (C-AgNPs) as capping agents. Thus, the understanding of the interaction between new antimicrobial agents and membranes (using model membranes as Langmuir monolayers and liposomes) represent a key aspect to elucidate their mechanism of action [38–40].

Synthesis of both G-AgNPs and C-AgNPs was visually observed by color change from colorless ($AgNO_3$ solution) to yellowish brown (AgNPs) and confirmed based on the UV–vis extinction spectra, which showed the typical extinction band between 350–450 nm attributed to

Table 1
Hydrodynamic size, polydispersity index, and zeta potential of AgNPs obtained by DLS. Measurements were conducted by setting the software as polydisperse distribution, but in all determination only one population was obtained (*i.e.* S.P Area Ratio:1). Polydispersity index informed correspond to the entry distribution. Values are presented as mean ± standard deviation (SD); n = 3 runs (each run correspond to 100 determinations).

Silver nanomaterial	Size (nm)	Polydispersity index	S.P Area Ratio	Zeta potential (mV)
G-AgNPs	46 ± 9	0.39	1	−22 ± 5
C-AgNPs	33 ± 3	0.17	1	−45 ± 5

the excitation of surface plasmon in these metal nanoparticles (Fig. 1A) [41]. A typical TEM micrograph indicates that the AgNPs obtained were almost spherical in shape and relatively uniform in diameter from 40 nm to 50 nm (Fig. 1B). The size distribution and an average nanoparticle size of AgNPs were obtained by DLS measurements (Fig. 1C, Table 1). The average size was found to be 46 nm and 33 nm for G-AgNPs and C-AgNPs, respectively. Moreover, the negative zeta potential values in Table 1 allow to indicate the reasonable stability of AgNPs in colloidal state and they prove evidence that the metal nanoparticles were dispersed in the medium.

The biophysical interaction of G-AgNPs with lipid surfaces was first studied by its effect on the surface pressure of lipid monolayers stabilized on the air-water interface. As revealed in Fig. 2A, the surface pressure changes increase as a function of the G-AgNPs concentration injected in the subphase in both pure DMPC or DMPC:DMPG monolayers. In addition, despite the net negative charge of G-AgNPs (see Table 1), it can be surprisingly observed that the highest pressure changes were found on negatively charged monolayers (PG containing) for a similar concentration of this nanomaterial. K_d and $\Delta\Pi_{max}$ values were determined in order to get an insight on the nature of AgNPs-lipid membrane interaction, fitting the experimental data from Fig. 2A with Eq. (1)(see Table 2). In agreement with the pointed above, the highest $\Delta\Pi_{max}$ and lowest K_d values were found for the membrane-mimetic model containing DMPG confirming the affinity between this lipid monolayer and G-AgNPs, both with net negative charge.

The kinetic behavior of the interaction event is shown in Fig. 2B, being the adsorption rate constant (k) obtained listed in Table 2. The kinetic results showed a faster G-AgNPs interaction on the DMPC:DMPG monolayer in comparison to that on the DMPC model, being the k value for green nanoparticles almost twice larger on negatively charged monolayers than on zwitterionic ones. Moreover, the fact that for both lipid compositions the value of n remains around 1 allow to indicate an interaction in independent sites. Again, these results indicate that G-AgNPs exhibited a higher affinity for DMPG-containing membranes than for zwitterionic ones. This is a very relevant result because DMPG

Table 2
Dissociation constant (k_d), heterogeneity parameter (n), $\Delta\Pi_{max}$, and adsorption rate constant (k) for green AgNPs-lipid monolayer interaction. Values were determined from surface pressure experiment by fitting data with Eqs. (1) and (2).

Lipid mixture	k_d	n	$\Delta\Pi_{max}$	k ($s^{-1} \times 10^{-4}$)^2
DMPC	0.21 ± 0.03	≅1	1.7 ± 0.2	3.51 ± 0.06
DMPC:DMPG (5:1)	0.13 ± 0.05	≅1	4.4 ± 0.3	6.07 ± 0.09

is the second major phospholipid component of bacterial plasma membranes [42]. In order to support that the effect on the lipid monolayers was due to the presence of G-AgNPs and not by the release of free silver ions in the solution, control experiments were carried out to evaluate the changes that silver ions are able to induce on the surface pressure. No significant pressure change was observed (data not shown). Similar experiments to those indicated above were conducted with AgNPs coated with citrate (C-AgNPs). However, in order to obtain comparable results of surface pressure changes, C-AgNPs concentrations at least twenty times higher were required (inset Fig. 2A). Moreover, the k_d values for both lipid compositions ((2.25 ± 0.18) for DMPC and (0.79 ± 0.03) for DMPC:DMPG) were higher than those obtained for green nanometals, indicating a lower affinity toward both membrane-mimetic models.

Antibacterial effect of both G-AgNPs and C-AgNPs was studied against representative Gram-positive and Gram-negative bacteria using the disk method. The results obtained show that G-AgNPs had a notable inhibitory activity of 12 mm and 14 mm against *S. aureus* and *E. coli*, respectively, and they were more bioactive than C-AgNPs similar in size and concentration, which showed negligible inhibition zones for both bacteria. To the best of our knowledge, this work constitutes the first biophysical analysis of the nanometal-membrane interaction that shows a clear correlation between membrane affinity/antibacterial activity and the chemical nature of capping ligands on the surface of AgNPs. Aromatic/hydrophobic moieties from chicoric and chlorogenic acids, as characteristic phenolic compounds present in the chicory extract [43], are expected on the green nanosilver surface; while, C-AgNPs were coated with aliphatic moieties when citrates adsorbed on the silver surface. The experimental results shows that both negatively charged-AgNPs could interact *via* electrostatic attraction with the polar heads of lipids, as was previously reported [16]. However, the aromatic/hydrophobic moieties adsorbed on G-AgNPs could play a relevance in the interactions with the hydrocarbon chain of lipids favoring a close contact of this nanomaterial with the lipid surface and facilitating its insertion into membrane [17,18]. This hydrophobic interaction for G-AgNPs should be responsible for their higher affinity toward bacteria-membrane mimetic systems than C-AgNPs, which could explain the strong antibacterial activity of G-AgNPs with respect to C-AgNPs.

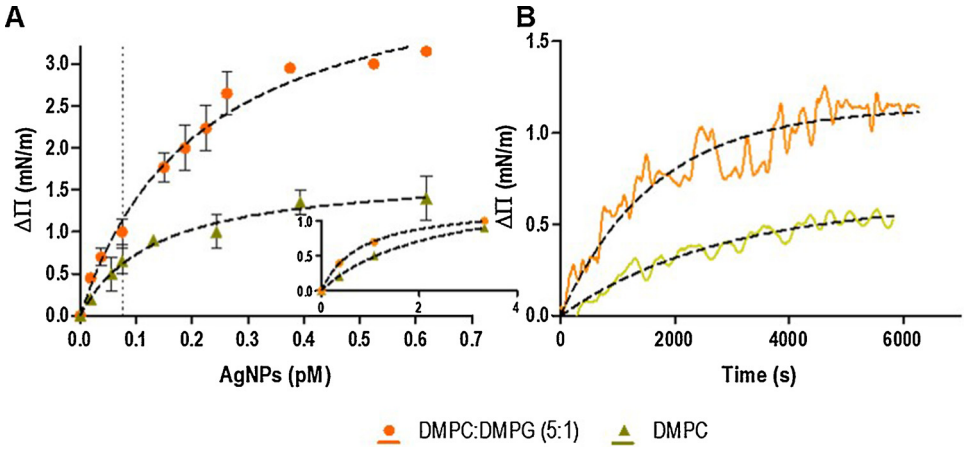

Fig. 2. A) Surface pressure changes as a function of G-AgNPs addition on DMPC or DMPC:DMPG monolayers. Continuous lines are fittings of Eq. (1) to the experimental data. The inset shows the surface pressure changes for the addition of C-AgNPs. B) Surface pressure changes as a function of time after addition of G-AgNPs to achieve a final concentration of 0.075 pM (dashed vertical line on Fig. 2A) on DMPC or DMPC:DMPG monolayers. All assays were carried out at 20 °C using an initial pressure of (20 ± 1) mN/m. Each point is the average of at least triplicates of independent samples.

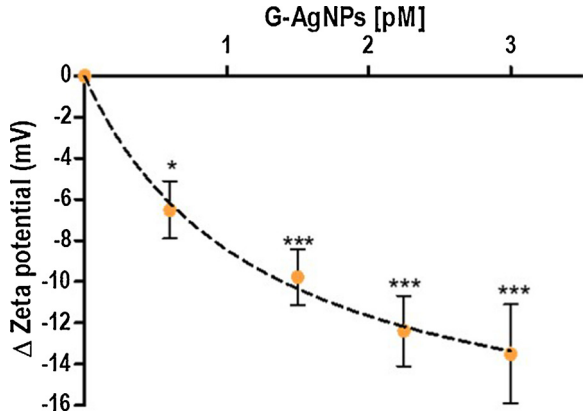

Fig. 3. Zeta potential values of DMPC:DMPG liposomes incubated with different concentrations of G-AgNPs. Each point represents the averages of twenty independent measurements in at least two different batches. Error bars indicate standard deviations of means. All assays were carried out at 20 °C. *, $P < 0.5$; ***, $P < 0.001$, one-way ANOVA followed by a Dunnett posttest for multiple comparisons *versus* the control column (without G-AgNps).

The available literature shows that electrostatic attraction between negatively charged-bacterial cells and positively charged-nanoparticles is crucial for the activity of nanoparticles as bactericidal agent [44,45]. However, the G-AgNPs evaluated in this study, despite being negatively charged (see Table 1), can somehow interact with the lipid membrane causing changes on the surface pressure as reported above. Considering that surface charges seem to be a key factor in the primary AgNPs-membrane interaction, zeta potential determinations were conducted using DMPC:DMPG (5:1) liposomes. Zeta potential data obtained are displayed in Fig. 3. It can be seen in this figure that the zeta potential of DMPC:DMPG liposomes become more negative with the addition of G-AgNPs as expected because of the net negative charge of this nanomaterial. These results confirm the interaction between the green nanoparticles and the lipid membrane, in an excellent agreement with previous surface pressure data. Furthermore, the fact that the net negative charge increases on the liposomes after incubation with G-AgNPs allows to indicate an interfacial interaction, where the nanoparticles or at least a portion of them *via* the insertion of aromatic/hydrophobic moieties of their surface-capping ligands, should be keep adsorbed to the membrane increasing negatively the liposomes charge.

Afterward, in order to confirm that the increase of zeta potential observed in Fig. 3 is the result of an interfacial adsorption of G-AgNPs on the membrane, DLS measurements were conducted on G-AgNPs, DMPC:DMPG liposomes (LUVs), and DMPC:DMPG liposomes incubated with G-AgNPs. As it can be seen in Fig. 4, pure liposomes and G-AgNPs exhibit a defined diameter peak of (46 ± 9) nm and (101 ± 15) nm, respectively. However, when liposomes were incubated with G-AgNPs a shift toward higher diameters ((220 ± 100) nm) was observed

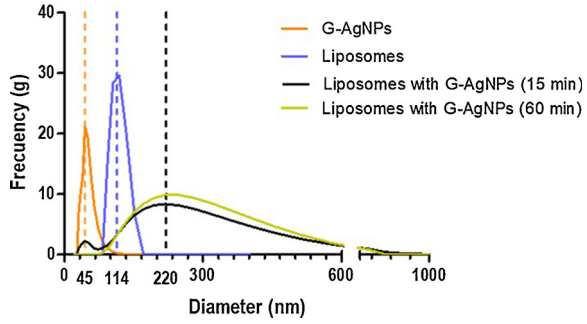

Fig. 4. Size distributions, obtained by DLS, of G-AgNPs, DMPC:DMPG liposomes, and liposomes in the presence of G-AgNPs after 15 and 60 min of incubation.

concomitant with the size change a more widespread distribution and an increase on polydispersion factor (from 0.15 ± 0.08 for liposomes to 0.41 ± 0.05 for liposomes with AgNPs) was observed, confirming a higher dispersion on particle sizes. Furthermore, at short incubation times (15 min), a small peak corresponding to pure G-AgNPs was observed which disappears at higher incubation times concomitant with an increase of the liposomes size ((257 ± 106) nm).

The explanation for this increase on the size of liposomes could be ascribed to an interfacial adsorption of the AgNPs, in good agreement with zeta potential measurements. The increase in liposomes size due to the adsorption of nanoparticles or peptides was previously reported [46,47]. It was previously reported that the size increase is related with the size of the nanomaterial [47], the fact that the AgNPs using in this study is relatively large (*i.e.* 50% of LUV size) could explain the dramatic size change. However, also another phenomenon could be involved in the size increase, as liposomal aggregation where the AgNPs would be a bridge between adjacent liposomes, thereby introducing interactions and thus accelerating their fusion or aggregation [48], or some others vesicle restructuring events. Overall, the obtained results confirm an interfacial interaction between AgNPs with liposomes.

Finally, in order to validate our observations in a real bacterial membrane, zeta potentials were determined to evaluate the ability of G-AgNPs to bind to the *E. coli* surface. As it can be observed in Fig. 5, 1 h of incubation with two different concentrations of G-AgNPs induces a significant decrease in the zeta potential values of *E. coli* confirming the capability of G-AgNPs to bind to the outer membrane of these bacteria, and the key role of the green nanosilver-lipid membrane interaction mediated by hydrophobic interactions as an essential step in the antibacterial mechanism of action of G-AgNPs either perturbing/modifying the lipid packing or acting as a local silver reservoir adsorbed that allows a higher toxic silver ions released into the bacterial cell [17,49].

4. Conclusions

In this work, a biophysical analysis using surface pressure, zeta potential, and DLS measurements allow probing that green negatively charged-AgNPs are able to interact with zwitterionic and negative lipid membranes *via* the insertion of aromatic/hydrophobic moieties of capping agents on the surface of G-AgNPs into lipids. Moreover, this research demonstrates for the first time that affinity toward lipid membranes is related with the antibacterial activity of G-AgNPs.

Beside further experiment should be made in order to fully characterization of mechanism of action of these green AgNPs, the results obtained in the present work allowed to claim that the interfacial interaction of this nanomaterial with bacterial membranes should be an

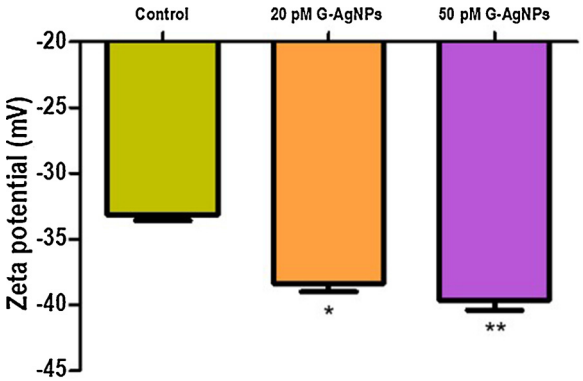

Fig. 5. Zeta potential values of *E. coli* incubated with different concentrations of G-AgNPs. Each point represents the averages of twenty independent measurements in at least three different batches. Error bars indicate standard deviations of means. All assays were carried out at 20 °C. *, $P < 0.5$; **, $P < 0.01$, one-way ANOVA followed by a Dunnett posttest for multiple comparisons *versus* the control column (without G-AgNPs).

essential step in the antibacterial activity either because the membrane is the main target or by allowing the accumulation of G-AgNPs thereby increasing the local concentration of silver that could lead then the bactericidal activity.

Furthermore, these findings relating membrane binding to the improved antibacterial potency of AgNPs, offer a rational basis for the application of green chemistry in the colloidal synthesis of new antimicrobial metal nanoparticles.

Acknowledgments

The authors wish to acknowledge the financial support of CONICET (PIP 11220130100702CO, PIP 11220130100383CO), CONICET-UNSE (PIO 14520140100013CO) and ANPCyT-FONCyT (PICT 2013-1482, PICT 2014-1663) from Argentina. PRD, BALM, and AH are members of the Research Career of CONICET. APVMF acknowledges fellowship from CONICET.

References

[1] C. Furusawa, T. Horinouchi, T. Maeda, Toward prediction and control of antibiotic-resistance evolution, Curr. Opin. Biotechnol. 54 (2018) 45–49, https://doi.org/10.1016/J.COPBIO.2018.01.026.

[2] L. Radlinski, B. Conlon, Antibiotic efficacy in the complex infection environment, Curr. Opin. Microbiol. 42 (2018) 19–24, https://doi.org/10.1016/J.MIB.2017.09.007.

[3] D.J. Diekema, K.J. Dodgson, B. Sigurdardottir, M.A. Pfaller, Rapid detection of antimicrobial-resistant organism carriage: an unmet clinical need, J. Clin. Microbiol. 42 (2004) 2879–2883, https://doi.org/10.1128/JCM.42.7.2879-2883.2004.

[4] M.K. Rai, S.D. Deshmukh, A.P. Ingle, A.K. Gade, Silver nanoparticles: the powerful nanoweapon against multidrug-resistant bacteria, J. Appl. Microbiol. 112 (2012) 841–852, https://doi.org/10.1111/j.1365-2672.2012.05253.x.

[5] A.F. Halbus, T.S. Horozov, V.N. Paunov, Colloid particle formulations for antimicrobial applications, Adv. Colloid Interface Sci. 249 (2017) 134–148, https://doi.org/10.1016/J.CIS.2017.05.012.

[6] W.K. Jung, H.C. Koo, K.W. Kim, S. Shin, S.H. Kim, Y.H. Park, Antibacterial activity and mechanism of action of the silver ion in *Staphylococcus aureus* and *Escherichia coli*, Appl. Environ. Microbiol. 74 (2008) 2171–2178, https://doi.org/10.1128/AEM.02001-07.

[7] J.S. McQuillan, H. Groenaga Infante, E. Stokes, A.M. Shaw, Silver nanoparticle enhanced silver ion stress response in *Escherichia coli* K12, Nanotoxicology 6 (2012) 857–866, https://doi.org/10.3109/17435390.2011.626532.

[8] B. Le Ouay, F. Stellacci, Antibacterial activity of silver nanoparticles: a surface science insight, Nano Today 10 (2015) 339–354, https://doi.org/10.1016/J.NANTOD.2015.04.002.

[9] M. Rai, K. Kon, A. Ingle, N. Duran, S. Galdiero, M. Galdiero, Broad-spectrum bioactivities of silver nanoparticles: the emerging trends and future prospects, Appl. Microbiol. Biotechnol. 98 (2014) 1951–1961, https://doi.org/10.1007/s00253-013-5473-x.

[10] M.A. Quinteros, I.M. Aiassa Martínez, P.R. Dalmasso, P.L. Páez, Silver nanoparticles: biosynthesis using an ATCC reference strain of *Pseudomonas aeruginosa* and activity as broad Spectrum Clinical antibacterial agents, Int. J. Biomater. 2016 (2016) 1–7, https://doi.org/10.1155/2016/5971047.

[11] W.-R. Li, X.-B. Xie, Q.-S. Shi, S.-S. Duan, Y.-S. Ouyang, Y.-B. Chen, Antibacterial effect of silver nanoparticles on Staphylococcus aureus, Biometals 24 (2011) 135–141, https://doi.org/10.1007/s10534-010-9381-6.

[12] E. Abbasi, M. Milani, S. Fekri Aval, M. Kouhi, A. Akbarzadeh, H. Tayefi Nasrabadi, P. Nikasa, S.W. Joo, Y. Hanifehpour, K. Nejati-Koshki, M. Samiei, Silver nanoparticles: synthesis methods, bio-applications and properties, Crit. Rev. Microbiol. (2014) 1–8, https://doi.org/10.3109/1040841X.2014.912200.

[13] M.N. Gallucci, J.C. Fraire, A.P.V. Ferreyra Maillard, P.L. Páez, I.M. Aiassa Martínez, E.V. Pannunzio Miner, E.A. Coronado, P.R. Dalmasso, Silver nanoparticles from leafy green extract of Belgian endive (Cichorium intybus L. var. sativus): Biosynthesis, characterization, and antibacterial activity, Mater. Lett. 197 (2017) 98–101, https://doi.org/10.1016/J.MATLET.2017.03.141.

[14] U.K. Parashar, V. Kumar, T. Bera, P.S. Saxena, G. Nath, S.K. Srivastava, R. Giri, A. Srivastava, Study of mechanism of enhanced antibacterial activity by green synthesis of silver nanoparticles, Nanotechnology 22 (2011) 415104, , https://doi.org/10.1088/0957-4484/22/41/415104.

[15] T.M. Nobre, F.J. Pavinatto, L. Caseli, A. Barros-Timmons, P. Dynarowicz-Łątka, O.N. Oliveira, Interactions of bioactive molecules & nanomaterials with Langmuir monolayers as cell membrane models, Thin Solid Films 593 (2015) 158–188, https://doi.org/10.1016/J.TSF.2015.09.047.

[16] F. Simonelli, D. Bochicchio, R. Ferrando, G. Rossi, Monolayer-protected anionic Au nanoparticles walk into lipid membranes step by step, J. Phys. Chem. Lett. 6 (2015) 3175–3179, https://doi.org/10.1021/acs.jpclett.5b01469.

[17] J. Gao, O. Zhang, J. Ren, C. Wu, Y. Zhao, Aromaticity/Bulkiness of surface ligands to promote the interaction of anionic amphiphilic gold nanoparticles with lipid bilayers, Langmuir 32 (2016) 1601–1610, https://doi.org/10.1021/acs.langmuir.6b00035.

[18] J.V. Maya Girón, R.V. Vico, B. Maggio, E. Zelaya, A. Rubert, G. Benítez, P. Carro, R.C. Salvarezza, M.E. Vela, Role of the capping agent in the interaction of hydrophilic Ag nanoparticles with DMPC as a model biomembrane, Environ. Sci. Nano 3 (2016) 462–472, https://doi.org/10.1039/C6EN00016A.

[19] R.L. Cruz Gomes da Silva, H.F. Oliveira da Silva, L.H. da, Silva Gasparotto, L. Caseli, How the interaction of PVP-stabilized Ag nanoparticles with models of cellular membranes at the air-water interface is modulated by the monolayer composition, J. Colloid Interface Sci. 512 (2018) 792–800, https://doi.org/10.1016/J.JCIS.2017.10.091.

[20] A. Hollmann, M. Martinez, M.E. Noguera, M.T. Augusto, A. Disalvo, N.C. Santos, L. Semorile, P.C. Maffia, Role of amphipathicity and hydrophobicity in the balance between hemolysis and peptide-membrane interactions of three related antimicrobial peptides, Colloids Surf. B Biointerfaces 141 (2016) 528–536, https://doi.org/10.1016/j.colsurfb.2016.02.003.

[21] P. Maturana, M. Martinez, M.E. Noguera, N.C. Santos, E.A. Disalvo, L. Semorile, P.C. Maffia, A. Hollmann, Lipid selectivity in novel antimicrobial peptides: implication on antimicrobial and hemolytic activity, Colloids Surf. B Biointerfaces 153 (2017) 152–159, https://doi.org/10.1016/j.colsurfb.2017.02.003.

[22] T.-H. Lee, C. Heng, M.J. Swann, J.D. Gehman, F. Separovic, M.-I. Aguilar, Real-time quantitative analysis of lipid disordering by aurein 1.2 during membrane adsorption, destabilisation and lysis, Biochim. Biophys. Acta - Biomembr. 1798 (2010) 1977–1986, https://doi.org/10.1016/J.BBAMEM.2010.06.023.

[23] J.T.J. Cheng, J.D. Hale, M. Elliott, R.E.W. Hancock, S.K. Straus, The importance of bacterial membrane composition in the structure and function of aurein 2.2 and selected variants, Biochim. Biophys. Acta - Biomembr. 1808 (2011) 622–633, https://doi.org/10.1016/J.BBAMEM.2010.11.025.

[24] A. Lorin, M. Noël, M.-È. Provencher, V. Turcotte, S. Cardinal, P. Lagüe, N. Voyer, M. Auger, Determining the mode of action involved in the antimicrobial activity of synthetic peptides: a solid-state NMR and FTIR study, Biophys. J. 103 (2012) 1470–1479, https://doi.org/10.1016/J.BPJ.2012.08.055.

[25] R. Pignatello, Drug-biomembrane Interaction Studies: The Application of Calorimetric Techniques, Elsevier, 2013.

[26] C, L.S. Institute, Performance Standards for Antimicrobial Disk Susceptibility Tests: Approved Standard, M02-A11 CLSI, Wayne (2012).

[27] T. Shireen, A. Basu, M. Sarkar, K. Mukhopadhyay, Lipid composition is an important determinant of antimicrobial activity of alpha-melanocyte stimulating hormone, Biophys. Chem. 196 (2015) 33–39, https://doi.org/10.1016/j.bpc.2014.09.002.

[28] T. Joshi, Z.X. Voo, B. Graham, L. Spiccia, L.L. Martin, Real-time examination of aminoglycoside activity towards bacterial mimetic membranes using Quartz Crystal Microbalance with Dissipation monitoring (QCM-D), Biochim. Biophys. Acta - Biomembr. 1848 (2015) 385–391, https://doi.org/10.1016/J.BBAMEM.2014.10.019.

[29] F. Nicol, S. Nir, F.C. Szoka, Effect of phospholipid composition on an amphipathic peptide-mediated pore formation in bilayer vesicles, Biophys. J. 78 (2000) 818–829, https://doi.org/10.1016/S0006-3495(00)76639-2.

[30] A.M. Bouchet, N.B. Iannucci, M.B. Pastrian, O. Cascone, N.C. Santos, E.A. Disalvo, A. Hollmann, Biological activity of antibacterial peptides matches synergism between electrostatic and non electrostatic forces, Colloids Surf. B Biointerfaces 114 (2014) 363–371, https://doi.org/10.1016/j.colsurfb.2013.10.025.

[31] L.D. Mayer, M.J. Hope, P.R. Cullis, Vesicles of variable sizes produced by a rapid extrusion procedure, Biochim. Biophys. Acta - Biomembr. 858 (1986) 161–168, https://doi.org/10.1016/0005-2736(86)90302-0.

[32] F. Szoka, F. Olson, T. Heath, W. Vail, E. Mayhew, D. Papahadjopoulos, Preparation of unilamellar liposomes of intermediate size (0.1–0.2 μm) by a combination of reverse phase evaporation and extrusion through polycarbonate membranes, Biochim. Biophys. Acta - Biomembr. 601 (1980) 559–571, https://doi.org/10.1016/0005-2736(80)90558-1.

[33] M.T. Augusto, A. Hollmann, M.A.R.B. Castanho, M. Porotto, A. Pessi, N.C. Santos, Improvement of HIV fusion inhibitor C34 efficacy by membrane anchoring and enhanced exposure infection, J. Antimicrob. Chemother. 69 (2014) 1286–1297, https://doi.org/10.1093/jac/dkt529.

[34] S.W. Provencher, A constrained regularization method for inverting data represented by linear algebraic or integral equations, Comput. Phys. Commun. 27 (1982) 213–227.

[35] S.W. Provencher, CONTIN: a general purpose constrained regularization program for inverting noisy linear algebraic and integral equations, Comput. Phys. Commun. 27 (1982) 229–242, https://doi.org/10.1016/0010-4655(82)90174-6.

[36] G. Grass, D.H. Nies, S. Franke, The product of the ybdE gene of the Escherichia coli chromosome is involved in detoxification of silver ions, Microbiology 147 (2001) 965–972, https://doi.org/10.1099/00221287-147-4-965.

[37] I. Sondi, B. Salopek-Sondi, Silver nanoparticles as antimicrobial agent: A case study on E. coli as a model for gram-negative bacteria, J. Colloid Interface Sci. 275 (2004) 177–182, https://doi.org/10.1016/j.jcis.2004.02.012.

[38] M.M. Domingues, R.G. Inacio, J.M. Raimundo, M. Martins, M.A. Castanho, N.C. Santos, Biophysical characterization of polymyxin B interaction with LPS aggregates and membrane model systems, Biopolymers 98 (2012) 338–344 http://www.ncbi.nlm.nih.gov/pubmed/23193598.

[39] M.M. Domingues, M.A.R.B. Castanho, N.C. Santos, rBPI(21) promotes lipopolysaccharide aggregation and exerts its antimicrobial effects by (hemi)fusion of PG-containing membranes, PLoS One 4 (2009) e8385, https://doi.org/10.1371/journal.pone.0008385.

[40] S. Troeira Henriques, M. Nuno Melo, M.A.R.B. Castanho, How to address CPP and AMP translocation? Methods to detect and quantify peptide internalization *in vitro* and *in vivo* (Review), Mol. Membr. Biol. 24 (2007) 173–184, https://doi.org/10.

1080/09687860601102476.
[41] E.A. Coronado, E.R. Encina, F.D. Stefani, Optical properties of metallic nanoparticles: manipulating light, heat and forces at the nanoscale, Nanoscale 3 (2011) 4042–4059, https://doi.org/10.1039/C1NR10788G.
[42] M.M. Domingues, S.C. Lopes, N.C. Santos, A. Quintas, M.A. Castanho, Fold-unfold transitions in the selectivity and mechanism of action of the N-terminal fragment of the bactericidal/permeability-increasing protein (rBPI(21)), Biophys. J. 96 (2009) 987–996, https://doi.org/10.1016/j.bpj.2008.10.044.
[43] Marzia Innocenti, Sandra Gallori, Catia Giaccherini, Francesca Ieri, Franco F. Vincieri, N. Mulinacci, Evaluation of the Phenolic Content in the Aerial Parts of Different Varieties of Cichorium intybus L. (2005), https://doi.org/10.1021/JF050541D.
[44] Peter K. Stoimenov, Rosalyn L. Klinger, George L. Marchin, Kenneth J. Klabunde, Metal Oxide Nanoparticles as Bactericidal Agents, (2002), https://doi.org/10.1021/LA0202374.
[45] T. Hamouda, J.R. Baker, Antimicrobial mechanism of action of surfactant lipid preparations in enteric gram-negative bacilli, J. Appl. Microbiol. 89 (2000) 397–403, https://doi.org/10.1046/j.1365-2672.2000.01127.x.
[46] A. Hollmann, L. Delfederico, N.C. Santos, E.A. Disalvo, Interaction of S-layer proteins of Lactobacillus kefir with model membranes and cells Interaction of S-layer proteins of Lactobacillus kefir with model membranes and cells, J. Liposome Res. 0 (2017) 000, https://doi.org/10.1080/08982104.2017.1281950.
[47] S. Savarala, S. Ahmed, M.A. Ilies, S.L. Wunder, Stabilization of Soft lipid colloids: competing effects of nanoparticle decoration and supported lipid bilayer formation, ACS Nano 5 (2011) 2619–2628, https://doi.org/10.1021/nn1025884.
[48] R. Michel, M. Gradzielski, Experimental aspects of colloidal interactions in mixed systems of liposome and inorganic nanoparticle and their applications, Int. J. Mol. Sci. 13 (2012) 11610–11642, https://doi.org/10.3390/ijms130911610.
[49] S. Eckhardt, P.S. Brunetto, J. Gagnon, M. Priebe, B. Giese, K.M. Fromm, Nanobio silver: its interactions with peptides and bacteria, and its uses in medicine, Chem. Rev. 113 (2013) 4708–4754, https://doi.org/10.1021/cr300288v.